Atmos. Chem. Phys. Discuss., 11, 6221–6258, 2011
www.atmos-chem-phys-discuss.net/11/6221/2011/
doi:10.5194/acpd-11-6221-2011

Atmospheric Chemistry and Physics Discussions

Optical properties of elemental carbon and water-soluble organic carbon in Beijing, China

Y. Cheng[1], K.-B. He[1], M. Zheng[2], F.-K. Duan[1], Y.-L. Ma[1], Z.-Y. Du[1], J.-H. Tan[1], J.-M. Liu[3], X.-L. Zhang[3], R. J. Weber[3], M. H. Bergin[3,4], and A. G. Russell[4]

[1]State Key Joint Laboratory of Environment Simulation and Pollution Control, Department of Environmental Science and Engineering, Tsinghua University, Beijing, China
[2]College of Environmental Sciences and Engineering, Peking University, Beijing, China
[3]School of Earth and Atmospheric Sciences, Georgia Institute of Technology, Atlanta, Georgia, USA
[4] School of Civil and Environmental Engineering, Georgia Institute of Technology, Atlanta, Georgia, USA

Received: 28 January 2011 – Accepted: 15 February 2011 – Published: 22 February 2011

Correspondence to: Y. Cheng (chengyuan02@gmail.com)

Published by Copernicus Publications on behalf of the European Geosciences Union.

Abstract

The mass absorption cross-section (MAC) of elemental carbon (EC) in Beijing was quantified using a thermal-optical carbon analyzer and the influences of mixing state and sources of carbonaceous aerosol were investigated. The MAC measured at 632 nm was 29.0 and 32.0 $m^2\,g^{-1}$ during winter and summer respectively. MAC correlated well with the organic carbon (OC) to EC ratio ($R^2 = 0.91$) which includes important information about the extent of secondary organic aerosol (SOA) production, indicating the enhancement of MAC by coating with SOA. The extrapolated MAC value was 10.5 $m^2\,g^{-1}$ when the OC to EC ratio is zero, which was 5.6 $m^2\,g^{-1}$ after correction by the enhancement factor (1.87) caused by the artifacts associated with the "filter-based" methods. The MAC also increased with sulphate ($R^2 = 0.84$) when the sulphate concentration was below 10 $\mu g\,m^{-3}$, whereas MAC and sulphate were only weekly related when the sulphate concentration was above 10 $\mu g\,m^{-3}$, indicating the MAC of EC was also enhanced by coating with sulphate. Based on a converting approach that accounts for the discrepancy caused by measurements methods of both light absorption and EC concentration, previously published MAC values were converted to the "equivalent MAC", which is the estimated value if using the same measurement methods as used in this study. The "equivalent MAC" was found to be much lower in the regions heavily impacted by biomass burning (e.g., India), probably due to the influence of brown carbon. Optical properties of water-soluble organic carbon (WSOC) in Beijing were also presented. Light absorption by WSOC exhibited strong wavelength (λ) dependence such that absorption varied approximately as λ^{-7}, which was characteristic of the brown carbon spectra. The mass absorption efficiency (σ_{abs}) of WSOC (measured at 365 nm) was 1.83 and 0.70 $m^2\,g^{-1}$ during winter and summer respectively. The seasonal pattern of σ_{abs} was attributed to the difference in the precursors of SOA, because WSOC in Beijing has been demonstrated to be strongly linked to SOA. Moreover, the σ_{abs} of WSOC in Beijing was much higher than results from the southeastern United States which were obtained using the same method as used in this study, perhaps due to the influence of biomass burning.

ACPD
11, 6221–6258, 2011

1 Introduction

Carbonaceous aerosol has been the focus of extensive studies during the last decade due to its complex effects on human health, visibility and climate change. Carbonaceous aerosol is an aggregate of thousands of poorly characterized species with a wide range of chemical, thermal and optical properties (Pöschl, 2005; Andreae and Gelencsér, 2006). As a result, its characterization is more difficult and complex compared with other components in ambient aerosol (e.g., sulphate and mineral dust). Though it is still impossible to completely identify carbonaceous aerosol on a molecular level, a variety of techniques has been developed to classify it into different fractions resulting in several "instrument-operational definitions" which are usually not congruent. In speciation monitoring, carbonaceous aerosol is commonly divided into organic carbon (OC) and elemental carbon (EC) by thermal-optical (or thermal) method (Chow et al., 1993; Birch and Cary, 1996). Another widely used definition is black carbon (BC), which is the light-absorbing carbon measured by optical instruments such as Aethalometer (Hansen and Novakov, 1990). In the emission-inventory and climate-science community, black carbon is usually used synonymously with EC, because the emission factors of BC are typically measured by thermal-optical (or thermal) methods. Recently, scientific attention has shifted from the role of black carbon as a pollutant to its importance as a driver of global warming (Jacobson, 2001; Ramanathan and Carmichael, 2008). Atmospheric heating caused by black carbon may affect the large scale circulation and the hydrological cycle with significant regional climate effects that contribute to the observed precipitation (increased summer floods in south China, increased drought in north China) and temperature (moderate cooling in China while most of the world has been warming) changes in China (Ramanathan et al., 2001; Menon et al., 2002).

The mass absorption cross-section (MAC, $m^2\,g^{-1}$), a parameter characterizing the optical properties of black carbon, is defined as:

$$\mathrm{MAC}\left(\mathrm{m}^2\,\mathrm{g}^{-1}\right) = \frac{b_{\mathrm{abs}}}{\mathrm{BC}} \quad (1)$$

ACPD
11, 6221–6258, 2011

where b_{abs} and BC is the absorption coefficient (Mm^{-1}) and mass concentration of black carbon ($\mu g\,m^{-3}$) respectively (Liousse et al., 1993). When calculating MAC by Eq. (1), EC measured by thermal-optical (or thermal) method is typically used as BC, and absorption measurements have most frequently been performed by "filter-based" techniques (e.g., Aethalometer) which measure the change in the light transmittance through a filter due to the deposition of airborne particles (Sharma et al., 2002; Jeong et al., 2004; Snyder and Schauer, 2007; Knox et al., 2009). However, significant artifacts are associated with the "filter-based" method, due to the aerosol-filter interactions, shadowing of the incident light with increasing filter loading, and aerosol scattering effects (Arnott et al., 2003; Weingartner et al., 2003; Petzold et al., 2005; Sandradewi et al., 2008). For example, results from downtown Toronto showed that the MAC value calculated based on Aethalometer was about 2.4 times the value based on photoacoustic spectrometer which can measure light absorption directly on airborne particles (Knox et al., 2009). Another concern in the determination of MAC is the influence of mixing state (Schnaiter et al., 2003, 2005; Bond et al., 2006). When BC is internally mixed with other components such as sulphate and organic carbon, the coatings can focus light into the BC core of the particle which would increase the MAC value (Bergstrom et al., 1982). Enhancement of MAC by coating can be described by absorption amplification. Laboratory studies showed that the amplification factor was $1.8 \sim 2.1$ for diesel soot particles when coated with secondary organic carbon produced by the oxidation of α-pinene (Schnaiter et al., 2005). The effects of coatings can also be evaluated by using a thermal-denuder which volatilizes the coatings (or a fraction of the coatings) by heating the airborne aerosol before absorption measurement. For example, Knox et al. (2009) found that the MAC of freshly emitted BC, which was calculated based on Aethalometer at 880 nm, was reduced by about 25% (from 19.3 to $14.4\,m^2\,g^{-1}$) after heating.

Black carbon is typically treated as the only light-absorbing species in climate models (Kirchstetter et al., 2004). However, it has been recently made clear that certain organic carbon species in addition to black carbon may also contribute to light absorption by

ACPD
11, 6221–6258, 2011

atmospheric aerosols, indicating a continuum of carbonaceous components (Pöschl, 2005; Andreae and Gelencsér, 2006). Light absorbing organic aerosol is usually termed brown carbon. Sources of brown carbon include residential coal combustion (Bond, 2001), biomass burning (Kirchstetter et al., 2004; Clarke et al., 2007; Bergstrom et al., 2007; Zhang et al., 2010), biogenic materials (Andreae and Crutzen, 1997), and atmospheric reactions (Gelencsér et al., 2003; Hecobian et al., 2010). Laboratory studies also provide additional evidence for the presence of brown carbon (Schnaiter et al., 2006; Chakrabarty et al., 2006, 2010). The "tar balls", which have been widely observed in Africa, Europe (Pósfai et al., 2004), North America (Hand et al., 2005) and Asia (Alexander et al., 2008), are considered as an important type of brown carbon. Though both can absorb light, "tar balls" differs substantially from black carbon in terms of morphology. "Tar balls" are large, amorphous, and predominantly isolated carbon spheres with diameter of 100 to 400 nm (Alexander et al., 2008), whereas black carbon typically consists of aggregates of spherules mostly 20 to 50 nm in diameter (van Poppel et al., 2005). The mass absorption efficiency of brown carbon increases sharply from long to short wavelengths, resulting in its brown appearance (Alexander et al., 2008). Absorption of ultraviolet (UV) light by brown carbon is important since UV irradiance significantly affects the tropospheric ozone production and photochemistry (Jacobson, 1999). Moreover, a significant fraction of brown carbon is water-soluble (Hoffer et al., 2006). Dissolution of brown carbon into cloud droplets could result in homogeneous absorbing droplets that affect the overall cloud absorption, especially in the UV range, indicating that brown carbon might have important influence on climate (Andreae and Gelencsér, 2006).

The radiative forcing of carbonaceous aerosol is one of the difficult challenges in climate modeling. Substantial uncertainties are due to the complexity in optical parameters of EC in the real atmosphere and the presence of light-absorbing organic carbon which is still poorly understood. In this study, optical properties of carbonaceous aerosol in Beijing, a representative mega city in East Asia, are presented. The MAC of EC is quantified using a thermal-optical carbon analyzer. Influence of source

ACPD
11, 6221–6258, 2011

and mixing state on the measured MAC values are investigated based on a converting approach that accounts for the discrepancy caused by the measurement methods of both light absorption and EC concentration. Moreover, light absorption characteristics of the $PM_{2.5}$ water extracts are also presented.

2 Methods

2.1 Field sampling

Ambient $PM_{2.5}$ samples were collected by a five-channel Spiral Ambient Speciation Sampler (SASS, MetOne Inc.) at the Tsinghua University campus in Beijing. Twenty-nine and thirty sets of daily $PM_{2.5}$ samples were collected during winter and summer, respectively, in 2009. Parallel quartz filters (denuded) and Teflon filters (un-denuded) were used in the present study. Detailed operating configuration of the SASS sampler during each sampling period was described by Cheng et al. (2010). The activated carbon denuder (provided by MetOne) is 20 mm long and 38 mm in diameter with about 1000 of 1 mm × 1 mm channels. A new denuder was used for each sampling campaign. Cheng et al. (2010) demonstrated that the denuder efficiency for removing the positive artifact was 100% throughout each sampling period. Particle loss due to diffusion to the walls of the denuder, volatilization of particulate organic carbon during transportation through the denuder, and the shedding of the denuder material were also shown to be negligible.

The quartz (2500 QAT-UP) and Teflon (R2PJ047) filters were from Pall Corp. (Ann Arbor, MI), and were 47 mm in diameter. The face velocity was 9.8 cm s^{-1} at the operating flow rate (6.7 L min^{-1}). All of the quartz and Teflon filters used throughout each campaign were taken from the same lot. The quartz filters were pre-baked at 550° in air for 24 h, whereas the Teflon filters were used as received from the manufacturer. Twenty-nine quartz filters were kept as filter blanks. The OC concentrations of the blank filters averaged 0.44 ± 0.15 μgC cm^{-2}, and no EC was detected. All of the data reported have been corrected by the filter blank concentration.

ACPD
11, 6221–6258, 2011

2.2 Sample analysis

2.2.1 Thermal-optical analysis

Quartz filters were analyzed using a DRI Model 2001 thermal/optical carbon analyzer (Atmoslytic Inc., Calabasas, CA) to determine the EC concentration and optical attenuation. The IMPROVE-A temperature protocol was implemented and EC was defined as the carbon evolved after the filter transmittance (monitored at 632,nm) returned to its initial value in the oxidizing atmosphere (He/O_2). The light attenuation caused by the presence of EC is defined as:

$$ATN = \ln\left(\frac{I_0}{I}\right) \quad (2)$$

where I and I_0 are the transmittance signal before and after the thermal-optical analysis. The determination of ATN is similar to that used in the Aethalometer, which simultaneously measures light passing through a loaded and a particle-free reference quartz filter. The absorption coefficient of the loaded aerosol (b_{abs}) is calculated as:

$$b_{abs}(Mm^{-1}) = ATN \times \frac{A}{V} \quad (3)$$

where A is the filter area with particle loading (mm^2) and V is the volume of air sampled (m^3). MAC is calculated as:

$$MAC\left(m^2\,g^{-1}\right) = \frac{b_{abs}}{EC} = \frac{ATN \times A}{EC \times V} = \frac{ATN}{EC_s} \times 10^2 \quad (4)$$

where EC_s ($\mu gC\,cm^{-2}$) is the filter loading of EC.

ACPD
11, 6221–6258, 2011

2.2.2 Water-soluble organic carbon and brown carbon analysis

Each Teflon filter was placed in a pre-cleaned 60 ml Nalgene amber HDPE bottle and extracted with 40 ml of 18-MΩ Milli-Q water via 30 min sonication. The liquid extract was then filtered using a 0.45 µm PTFE syringe filter and then stored in a refrigerator (~4°) until analysis, which was completed within 2 days after extraction. Sulphate and water-soluble organic carbon (WSOC) in the extract was quantified using an Ion Chromatography (Dionex-600) and a Sievers Model 900 Total Organic Carbon Analyzer (GE Analytical Instruments, Boulder, CO) respectively.

The light absorption spectra of the liquid extracts were measured over the wavelength range of 250 to 800 nm with a UV-Visible Spectrophotometer and Long-Path Absorption Cell, following the method of Hecobian et al. (2010). Water extracts were injected into a 1-m path-length Liquid Waveguide Capillary Cell (LWCC-2100, World Precision Instrument, Sarasota, FL) with an internal volume of 250 µL. A dual deuterium and tungsten halogen light source (DT-Mini-2, Ocean Optics, Dunedin, FL) and absorption spectrometer (USB4000, Ocean Optics, Dunedin, FL) were coupled to the wave-guide via fiber optic cables (QP400-2-SR, Ocean Optics, Dunedin, FL). The absorption spectra were recorded with an Ocean Optics Spectra-Suite data acquisition system.

Light absorption of the liquid extracts is defined as:

$$\mathrm{ATN}_\lambda = -\log_{10}\left(\frac{I}{I_0}\right) = L \times \sum\nolimits_i (C_i \times \varepsilon_{i,\lambda}) \quad (5)$$

where I_0 and I are the intensity of incident and transmitted light respectively. ATN_λ is linearly dependent on the concentration of light-absorbing substances in solution (C_i), their wavelength-dependent mass absorption coefficient ($\varepsilon_{i,\lambda}$), and the absorbing path length (L). ATN_λ is then converted to an absorption coefficient $(b_{\mathrm{abs}})_\lambda$ by:

$$(b_{\mathrm{abs}})_\lambda = (\mathrm{ATN}_\lambda - \mathrm{ATN}_{700}) \times \frac{V_{\mathrm{W}}}{V \times L} \times \ln(10) \quad (6)$$

ACPD
11, 6221–6258, 2011

where V_W is the volume of water into which the filter was extracted (40 ml), V is the volume of air sampled, and L is the absorbing path length (0.94 m). Absorbance at 700 nm (average between 695 and 705 nm, where there is no absorption for ambient aerosol water extracts) is used to account for baseline drift during analysis. Ln (10) converts from common logarithm (base 10) to natural logarithm. The mass absorption efficiency $(\sigma_{abs})_\lambda$ of the water extracts is calculated as:

$$(\sigma_{abs})_\lambda = \frac{(b_{abs})_\lambda}{WSOC} \quad (7)$$

3 Results and Discussion

3.1 Optical properties of elemental carbon

The dependence of light attenuation measured at 632 nm (ATN) on EC loading (EC_s, $\mu gC\,cm^{-2}$) is shown in Fig. 1. During the winter, ATN and EC_s correlated well (R^2 = 0.915) with a slope of 29.0 $m^2\,g^{-1}$ and an intercept of 5.7 $m^2\,g^{-1}$ when the EC_s was below 7 $\mu gC\,cm^{-2}$, whereas the linearity did not extend for EC_s exceeding 7 $\mu gC\,cm^{-2}$ due to the shadowing effect. During the summer, EC_s was much lower (below 4 $\mu gC\,cm^{-2}$) and ATN was less variable; regression between ATN and EC_s showed a slope of 32.0 $m^2\,g^{-1}$ and an intercept of 4.8 $m^2\,g^{-1}$ (R^2 = 0.604). The relatively low intercept values obtained in this study indicated that EC was the major light-absorbing component of $PM_{2.5}$ in Beijing.

3.2 Effects of the measurement methods

Previous studies have quantified the MAC by the "filter-based" method at a variety of locations (Table 1). However, quite different measurement methods of both ATN and EC_s have been implemented, introducing complexity and difficulty in the direct comparison of MAC across studies and regions. As a result, an approach was developed

ACPD
11, 6221–6258, 2011

to account for the discrepancy caused by measurements methods of both ATN and EC_s. Based on this approach, previously reported MAC values were converted to the "equivalent MAC", which is the estimated value if using the same measurement methods (of both ATN and EC_s) as used in this study. This was done using the following procedures.

(1) EC method conversion. The thermal-optical method is widely used for the determination of EC. A variety of operational protocols have been employed that differ mainly with respect to (i) temperature protocol, including temperature plateaus and residence time at each plateaus, and (ii) charring correction by light reflectance or transmittance. EC values defined by transmittance correction (EC_T) are usually lower than those defined by reflectance correction (EC_R), because the filter reflectance signal typically returns to its initial value before the transmittance (Chow et al., 2004). Influence of the charring correction methods on EC values is shown in Table 2. When using the IMPROVE or the IMPROVE-A temperature protocol, the EC_R to EC_T ratio was about $1.3 \sim 1.8$ for ambient samples whereas the ratio was a little lower (about 1.2) for motor vehicle exhaust samples. As a result, when converting MAC values in which EC was determined by the IMPROVE (or IMPROVE-A) temperature protocol with reflectance correction, the reported MAC was multiplied by $1.3 \sim 1.8$ to account for the discrepancy caused by charring correction methods. On the other hand, the EC_R to EC_T ratio varied significantly (by a factor of more than 3) when the NIOSH or similar temperature protocol (STN) was used (Table 2), perhaps due to the influence of "early split" which means the reflectance or transmittance signal returns to its initial value before the introduction of O_2. "Early split" is usually caused by the high peak inert mode temperature (e.g., 870° and 900 ° used in NIOSH and STN protocol) which might result in the premature evolution of light-absorbing carbon (Sciare et al., 2003; Subramanian et al., 2006; Cheng et al., 2010). "Early split" occurs more frequently for the reflectance signal. For example, it happens in about 80% and 40% of the Fresno samples when using the reflectance and transmittance correction respectively (the temperature protocol was STN); and the EC_R to EC_T ratio was as high as about 3.5 (Chow et al., 2004). In case

ACPD
11, 6221–6258, 2011

of "early split", all of the carbon involved in the He/O_2 mode would be classified as EC. If "early split" occurs for both the reflectance and transmittance signal, EC_R would be the same as EC_T, which may be the case for the Mexico urban samples (Table 2). As a result, we do not suggest conversion between EC_R and EC_T when using the NIOSH or similar temperature protocols that may be complicated by the "early split".

Measured EC values have also been shown to vary significantly among the various temperature protocols (Schauer et al., 2003; Subramanian et al., 2006; Cheng et al., 2010). Based on results from North America and Europe, ambient EC defined by the IMPROVE temperature protocol ($EC_{IMPROVE}$) was about $1.2 \sim 1.5$ times the value of that defined by NIOSH (EC_{NIOSH}) when both using the transmittance correction (Cheng et al., 2010 and references therein). Few studies about the $EC_{IMPROVE}$ to EC_{NIOSH} ratio were available for Asia and quite different results have been reported. Results from Schauer et al. (2003) suggested that the ratio was about 1.5 for a regional background site in Korea whereas recent work by Cheng et al. (2010) indicated that the ratio may be greater than 2.0 for Beijing, China. Importantly, the discrepancy between EC values determined by different methods was suggested to be strongly linked to brown carbon such that the discrepancy was larger when the contribution of brown carbon was high (Reisinger et al., 2008). As a result, the $EC_{IMPROVE}$ to EC_{NIOSH} ratio for Asia is expected to be higher than that for North America and Europe, due to the much stronger emissions from the biomass burning and residential coal combustion (Bond et al., 2004; Venkataraman et al., 2005; Gustafsson et al., 2009) which are known to emit large amounts of brown carbon. When converting the MAC values in which EC was determined by the NIOSH temperature protocol with transmittance correction, different converting factors were used to account for the discrepancy caused by the temperature protocol: if the reported MAC was measured in North America or Europe, it was divided by $1.2 \sim 1.5$; if the reported MAC was measured in Asia, it was divided by 1.5 to obtain upper estimate of the "equivalence MAC".

ACPD
11, 6221–6258, 2011

(2) Wavelength measurement correction. The wavelength (λ) dependence of MAC can be represented as a power-law relationship using an Ångstrom exponent (Å):

$$\mathrm{MAC}_{\lambda} = K \times \lambda^{-\text{Å}} \tag{8}$$

where K is a constant that includes the aerosol mass concentration. A value of Å = 1 was used for the present study. Then MAC measured at a given wavelength (MAC_{λ}) could be converted to that measured at 632 nm (MAC_{632}) by Eq. (9):

$$\mathrm{MAC}_{632} = \mathrm{MAC}_{\lambda} \times \frac{\lambda}{632} \tag{9}$$

After incorporating the EC method conversion and the wavelength measurement correction, the whole converting approach to calculate the "equivalent MAC" from reported values is:

$$\text{equivalent MAC} = \mathrm{MAC}_{\lambda} \times \frac{\lambda}{632} \times \frac{f_{\text{charring}}}{f_{\text{protocol}}} \tag{10}$$

where λ is the wavelength at which the reported MAC is measured; f_{charring} is the converting factor of charring correction method, $f_{\text{charring}} = 1.3 \sim 1.8$ for reported MAC in which EC was determined by the IMPROVE (or IMPROVE-A) temperature protocol with reflectance correction; f_{protocol} is the converting factor of temperature protocol, $f_{\text{protocol}} = 1.2 \sim 1.5$ or 1.5 for reported MAC in which EC was determined by the NIOSH temperature protocol (or similar protocol such as STN) with transmittance correction, depending on where the reported MAC was measured.

Effects of the converting approach on the reported MAC values depend on the measurement methods of both light absorption and EC concentration. As shown in Table 1, if the reported MAC were calculated by ATN measured at a wavelength greater than 632 nm (e.g., 880 nm) together with EC defined by the IMPROVE temperature protocol with reflectance correction, the "equivalent MAC" would be substantially higher than the reported value, because the reported MAC would be increased by both the

ACPD
11, 6221–6258, 2011

EC method conversion and the wavelength measurement correction process. In this case, the discrepancy between the reported MAC and the values obtained in this study would be reduced. For example, it seems that MAC values obtained in this study were about 1 ~ 2 times higher than those reported by Babich et al. (2000); but the converting approach increased the reported MAC values by a factor of 1.8 ~ 2.5, indicating the MAC values reported by Babich et al. (2000) were in fact comparable with results from this study. However, the converting approach has little influence on the reported MAC values which were quantified by ATN measured at 880 nm together with EC defined by the NIOSH temperature protocol with transmittance correction, because of the opposite effects of the EC method conversion and the wavelength measurement correction. The converting approach might also induce a larger discrepancy between the reported MAC values and results from this study. For example, MAC measured at a high-altitude site in India (Manora Peak, 24.7 $m^2\,g^{-1}$) seems only a little lower compared to the value obtained in Beijing during the same season (29.0 $m^2\,g^{-1}$); but after accounting for the influence of measurement methods, the reported value was in fact less than 60% of that in Beijing.

3.3 Effects of aerosol composition and sources

Other factors in addition to measurement methods that influence MAC values can be investigated based on the converting approach described above, which would provide deep insight into the optical properties of elemental (or black) carbon. The "equivalent MAC" shown in Table 1 could be classified into three groups according to their values. The first group includes an extremely high value (55.6 ~ 69.5 $m^2\,g^{-1}$) measured in Philadelphia, PA during severe sulphate haze episodes occurred in the summer of 2002 (Jeong et al., 2004), and also includes results from Beijing (this study) and seven American cities. In the first group, the upper estimates of the "equivalent MAC" were above (or close to) 30 $m^2\,g^{-1}$, and the lower estimates were above 20 $m^2\,g^{-1}$. The second group consists of eight "equivalent MAC" values measured in North America and Europe. In this group, the upper and lower estimates of the "equivalent MAC"

ACPD
11, 6221–6258, 2011

were between 21 ~ 26 and 15 ~ 21 $m^2\,g^{-1}$ respectively. The third group comprises results from Asia and those measured in North America and Europe during the periods impacted by biomass burning. The "equivalent MAC" values of this group were significantly lower. For example, the "equivalent MAC" measured in Philadelphia, PA during a Canadian forest fire event was only between 5.4 ~ 6.7 $m^2\,g^{-1}$ (Jeong et al., 2004).

In a recent review, Bond and Bergstrom (2006) suggested a value of 7.5 $m^2\,g^{-1}$ for MAC of uncoated elemental carbon at 550 nm, which was 6.5 $m^2\,g^{-1}$ after accounting for the measurement wavelength by Eq. (9). As shown in Table 1, most of the "equivalent MAC" values were significantly higher than 6.5 $m^2\,g^{-1}$. The discrepancy could be attributed to three factors. The first is the enhancement of MAC due to the artifacts associated with the "filter-based" methods. A generally valid correction scheme for the enhancement effect is presently not available. One of the commonly used approaches was developed by Weingartner et al. (2003):

$$\mathrm{MAC}_{\mathrm{corrected}} = \frac{\mathrm{MAC}}{C \times R(\mathrm{ATN})} \tag{11}$$

The factor C is used to correct for multiple scattering within a relatively clean filter. A value of $C = 2.14$ was suggested by Weingartner et al. (2003) for the same type of quartz filter as used in this study. $R(\mathrm{ATN})$ corrects for the shadowing effect, which is empirically defined as:

$$R(\mathrm{ATN}) = \left(\frac{1}{f} - 1\right) \times \frac{\ln(\mathrm{ATN}) - \ln(10\%)}{\ln(50\%) - \ln(10\%)} + 1 \tag{12}$$

Based on ATN values obtained in this study, $R(\mathrm{ATN})$ was 0.87 ± 0.05 and 0.87 ± 0.03 during winter and summer respectively, if using f values of 1.103 for winter and 1.114 for summer (Sandradewi et al., 2008). As a result, the enhancement factor, $C \times R(\mathrm{ATN})$, averaged 1.87 ± 0.11 and 1.87 ± 0.06 during winter and summer respectively. Comparably, Knox et al. (2009) found that the enhancement factor was about 2.4 based on comparison between results from Aethalometer and photoacoustic spectrometer. The

ACPD
11, 6221–6258, 2011

second factor is the uncertainties in the thermal-optical measurement of EC. It has been demonstrated that EC concentration would be under-estimated by the value that is operationally-defined by the thermal-optical method (with transmittance correction, Chow et al., 2004; Subramanian et al., 2006; Cheng et al., 2009), which was referred to as the "systemic artifact" of thermal-optical method by Cheng et al. (2010). As far as we know, only Chow et al. (2004) and Cheng et al. (2009) quantitatively assessed the under-estimation of EC due to the "systemic artifact". However, both studies were based on a small number of samples collected at a single sampling site (31 Fresno samples and 20 Beijing samples, respectively). As a result, a reliable factor that accounts for the "systemic artifact" is still not available. The third factor is the enhancement of MAC by coating with sulphate and /or organic carbon. Though not all of the sulphate is necessarily internally-mixed with EC, the relationship between MAC and the concentration of airborne sulphate could provide some valuable information about the effects of sulphate on the optical properties of EC. As shown in Fig. 2, the presence of sulphate increased the MAC when the sulphate concentration was below 10 $\mu g\,m^{-3}$, whereas MAC and sulphate were only weekly related when the sulphate concentration was above 10 $\mu g\,m^{-3}$. Figure 2 indicates that sulphate is probably internally-mixed with EC during summertime in Beijing and the enhancement of MAC due to coating with sulphate might not be significant beyond a certain coating thickness which is consistent with the theoretical predictions of Bond et al. (2006). Moreover, the extrapolated MAC value was 22.4 $m^2\,g^{-1}$ when the sulphate concentration was zero, which was still much higher than that of uncoated EC (6.5 $m^2\,g^{-1}$) suggested by Bond and Bergstrom (2006), even after considering the enhancement factor of MAC (1.87) due to the artifacts associated with the "filter-based" methods. The most likely cause is that other species in addition to sulphate also build up on EC. OC is another component in ambient aerosol that would be internally-mixed with EC, and laboratory studies have demonstrated that coating with OC would increase the MAC value of EC (Schnaiter et al., 2003, 2005). However, as shown in Fig. 3a, MAC only showed a moderate correlation with the OC concentration ($R^2 = 0.530$), suggesting that enhancement of MAC caused by coating

ACPD
11, 6221–6258, 2011

with OC does not seem significant. But it should be kept in mind that OC comprises both primary organic carbon (POC) that is directly emitted from combustion sources and secondary organic carbon (SOC) that is formed through atmospheric oxidation, either homogeneous or inhomogeneous. Moreover, SOC might be more likely to build up on EC, especially when the inhomogeneous oxidation is important. This hypothesis was strongly supported by the high correlation ($R^2 = 0.910$) between MAC and the OC to EC ratio which includes important information about the extent of secondary organic aerosol (SOA) production (Cheng et al., 2011, Fig. 3b). Figure 3b indicated that the enhancement of MAC is strongly linked to the coating by SOA. Moreover, the MAC of uncoated EC can be estimated as the extrapolated value when the OC to EC ratio is zero, which was $10.50\,m^2\,g^{-1}$. After correction by the enhancement factor (1.87) caused by the artifacts associated with the "filter-based" methods, the estimated MAC of uncoated EC was $5.6\,m^2\,g^{-1}$, which is comparable with the value suggested by Bond and Bergstrom (2006).

The discussion above indicated that the unrealistically high values of MAC in Table 1 are mainly due to the artifacts associated with the "filter-based" methods and the enhancement by the coating with both sulphate and secondary organic carbon. Table 3 shows the upper and lower estimates of the "equivalent MAC" values of the three groups which have been corrected for the artifacts associated the "filter-based" methods. In the first group, the corrected "equivalent MAC" values ($11 \sim 21\,m^2\,g^{-1}$) were about $1 \sim 2$ time higher than the suggested value ($6.5\,m^2\,g^{-1}$) of uncoated EC (Bond and Bergstrom, 2006), indicating MAC values in this group were significantly enhanced by coating. In the second group, the corrected "equivalent MAC" values were in the range of $8 \sim 14\,m^2\,g^{-1}$, indicating moderate enhancement by coating.

The "equivalent MAC" values in the third group were much lower. The MAC of EC in two Indian cities (Hisar and Allahabad), which were calculated by a similar method as used in this study, were less than 50% of that in Beijing during the same season (Sam and Sarin, 2009), suggesting EC in India was significantly less light-absorbing. The observed difference in optical properties indicates that the sources of EC were quite

ACPD
11, 6221–6258, 2011

different in China than India. EC in India has been shown to be dominated by emissions from biomass burning (Venkataraman et al., 2005; Gustafsson et al., 2009), whereas coal burning (both industry and residential) is the largest source of EC emission in China (Bond et al., 2004; Cao et al., 2006). Biomass burning is known to emit a significant amount of brown carbon that can not be directly measured by the currently-used thermal-optical equipments. A fraction of brown carbon might be classified as EC, resulting in an artifact that increases the mass concentration of EC. On the other hand, the presence of brown carbon would not significantly influence the value of ATN, which is usually measured at wavelengths greater than 500 nm (Table 1). According to Eq. (4), brown carbon is expected to decrease the value of MAC, indicating that the large amount of brown carbon in the atmosphere of India, which is emitted from biomass burning, is the most likely factor causing its significantly lower MAC values comparing with other regions. The hypothesis was further supported by results from North America and Europe such that the reported MAC values were much lower during the periods impacted by biomass burning (Allen et al., 1999; Jeong et al., 2004; Krecl et al., 2007). As a result, the relatively low values of MAC in the third group were most likely due to the presence of brown carbon or the influences of biomass burning.

3.4 Optical properties of water-soluble organic carbon

WSOC averaged 7.3 and 3.4 $\mu gC\,m^{-3}$, and constituted 22% and 39% of OC (measured by the denuded quartz filter), during winter and summer respectively (Cheng et al., 2011). The light absorption spectra over the wavelength range of 250 to 800 nm were recorded for the liquid extracts. The power law fit well in the wavelength range of 330–480 nm as shown in Fig. 4. The Ångstrom exponents calculated by Eq. (8) averaged 7.5 ± 0.9 and 7.0 ± 0.8 during winter and summer respectively. The Ångstrom exponents were similar to those of humic-like substances (HULIS) isolated from the ambient aerosol in Amazonian biomass burning plumes (Hoffer et al., 2006), and are also comparable with those of the water extracts measured in the southeastern United States (Hecobian et al., 2010). The absorption spectra observed for the WSOC (Fig. 4)

ACPD
11, 6221–6258, 2011

is characteristic of the brown carbon spectra with a sharply increasing absorption when wavelength decreases ($\sigma_{abs} \sim \lambda^{-7}$), which strongly supports that WSOC (or a fraction of WSOC) obtained in this study is brown carbon. In fact, a significant quantity of evidence for the atmospheric presence of brown carbon comes from the spectral properties of water extracts of continental aerosol (Andreae and Gelencsér, 2006; Lukács et al., 2007). Recently, a fraction of brown carbon was found to be non-water-soluble (Chen and Bond, 2010), but this fraction was not the focus of this study.

Though the light absorption spectra were recorded from 250 to 800 nm, the absorption coefficient (b_{abs}) and mass absorption efficiency (σ_{abs}) of WSOC were calculated at 365 nm (average between 360 and 370 nm) by Eqs. (5) to (7). This wavelength was chosen to avoid interferences from non-organic compounds such as nitrate and to maintain consistency with previously published results (Lukács et al., 2007; Hecobian et al., 2010). During the winter, b_{abs} and WSOC correlated well with a slope of $1.83 \pm 0.03\,m^2\,g^{-1}$ ($R^2 = 0.977$), whereas the regression between b_{abs} and WSOC showed a slope of $0.70 \pm 0.03\,m^2\,g^{-1}$ during the summer ($R^2 = 0.734$, Fig. 5). Cheng et al. (2011) found that WSOC correlated well ($R^2 = 0.84 \sim 0.94$) with the secondary organic aerosol (SOA) predicted by the EC-tracer method, indicating a substantial fraction of WSOC is SOA in Beijing; moreover, the estimated SOA accounted for about 40 and 50% of organic aerosol (OA, measured by the denuded quartz filter) during winter and summer respectively, suggesting considerable SOA production despite the low temperature in winter. Importantly, the emission of biogenic volatile organic compounds (BVOCs) in Beijing showed a distinct seasonal pattern such that the BVOCs emission reached a maximum in summer (e.g., 4.4×10^9 gC in July) whereas the emission was much lower during winter (e.g., 6.3×10^6 gC in January, Wang et al., 2003). As a result, anthropogenic volatile organic compounds (AVOCs) should be more important as the precursors of SOA during winter compared with summer. Given the fact that WSOC is strongly linked to SOA in Beijing, the difference in the precursors of SOA is a most likely cause of the discrepancy in the σ_{abs} of WSOC during winter and summer.

ACPD
11, 6221–6258, 2011

Previous studies suggested that biomass burning is another source of WSOC (Sullivan et al., 2006; Weber et al., 2007; Snyder et al., 2009). Effects of biomass burning on the σ_{abs} of WSOC could be illustrated by results from Hecobian et al. (2010). In the southeastern United States, the σ_{abs} (measured at 365 nm using the same method as used in this study) were 0.31 $m^2\,g^{-1}$ (0.21 ~ 0.42 $m^2\,g^{-1}$) and 0.29 (0.26 ~ 0.32m^2/g) for urban and rural sites respectively, when the contribution of biomass burning was not important (identified by levoglucosan <50 ng m^{-3}, typically in the summer); whereas the σ_{abs} averaged 0.70 $m^2\,g^{-1}$ (0.62 ~ 0.84 $m^2\,g^{-1}$) and 0.62 (0.57 ~ 0.67 $m^2\,g^{-1}$) for urban and rural sites respectively, when the influence of biomass burning was significant (identified by levoglucosan >50 ng m^{-3}, typically in the winter and spring). These results seem to indicate that WSOC emitted from biomass burning is more light-absorbing compared with that formed by atmospheric reaction. This hypothesis was supported by the much higher σ_{abs} value in Beijing (0.70 ~ 1.83 $m^2\,g^{-1}$) where the levoglucosan concentration was above 100 ng m^{-3} all year round (averaging 307 ng/m^3, Zhang et al., 2008). The high levoglucosan concentration throughout the year was mainly due to the agricultural waste and firewood that is commonly consumed as domestic fuel in the rural areas of Beijing as well as in neighboring provinces, which resulted in a background contribution of biomass burning to Beijing aerosol existing throughout the year (Zhang et al., 2008). Moreover, Beijing might also be heavily impacted by the open burning of agricultural waste in nearby provinces (open burning is prohibited in Beijing), which was significant only in the harvest season such as early summer when wheat is harvested and autumn when maize is harvested (Duan et al., 2004; He et al., 2006; Zhang et al., 2008; Li et al., 2010). Recent results from source apportionment by CMB (chemical mass balance) suggested that biomass burning accounted for 11 and 26% of ambient OC in Beijing during summer (not within the period when wheat is harvested) and winter respectively, which was consistent with the levoglucosan to OC ratio (0.6 and 1.4% during summer and winter respectively, Wang et al., 2009). The higher contribution in winter, when there are no harvest activities, should be due to the large amount of biofuels used for domestic heating in northern

ACPD
11, 6221–6258, 2011

China. On the other hand, He et al. (2006) found that the levoglucosan to OC ratio was comparable (about 0.2%) during winter and summer (not within the harvest season), indicating the contribution of biomass burning to ambient OC in Beijing was comparable during winter and summer. A similar seasonal pattern of the levoglucosan to OC ratio was also found by Zhang et al. (2008). These results suggest that the biomass burning contribution and its seasonal pattern is still highly uncertain for the Beijing region. Given the fact that the WSOC in Beijing was dominated by SOA during both winter and summer (Cheng et al., 2011), it could only be concluded that biomass burning might be responsible for the much higher absolute value of σ_{abs} in Beijing comparing with the southeastern United States; whether it contributes to the seasonal variation of σ_{abs} in Beijing is still inconclusive.

4 Conclusions

The MAC of EC in Beijing was quantified using a thermal-optical carbon analyzer. The absorption measurement was performed at 632 nm and the EC concentration was determined by the IMPROVE-A temperature protocol with transmittance charring correction. The MAC was 29.0 and 32.0 $m^2\,g^{-1}$ during winter and summer respectively. The unrealistically high MAC values were mainly due to two factors. The first is the artifacts associated with the "filter-based" methods, such as the multiple scattering within a relatively clean filter and the shadowing effect. The enhancement factor was 1.87, which was calculated following Weingartner et al. (2003) and Sandradewi et al. (2008). The second is the enhancement of MAC by coating. MAC correlated well with the OC to EC ratio ($R^2 = 0.91$) which includes important information about the extent of secondary organic aerosol (SOA) production, indicating the enhancement of MAC by coating with SOA. The MAC value also increased with sulphate ($R^2 = 0.84$) when the sulphate concentration was below 10 $\mu g\,m^{-3}$. However, MAC and sulphate were only weekly related when the sulphate concentration exceeding 10 $\mu g\,m^{-3}$. The extrapolated MAC value was 10.5 $m^2\,g^{-1}$ when the OC to EC ratio is zero, which was comparable with the value

ACPD
11, 6221–6258, 2011

suggested for uncoated EC (6.5 $m^2\,g^{-1}$, Bond and Bergstrom, 2006) after correction by the enhancement factor (1.87) caused by the artifacts associated with the "filter-based" methods. On the other hand, the extrapolated MAC value was 22.4 $m^2\,g^{-1}$ when the sulphate concentration is zero, which was still significantly higher than the suggested value of uncoated EC even after accounting for the artifacts associated with the "filter-based" methods. These results indicated that the MAC of EC in Beijing was enhanced by the coating with both SOA and sulphate, and the enhancement was more strongly linked to SOA.

A converting approach, including the EC method conversion and the wavelength measurement correction, was developed to account for the discrepancy caused by measurements methods of both light absorption and EC concentration. Based on this approach, previously published MAC values were converted to the "equivalent MAC", which is the estimated value if using the same measurement methods (of both ATN and EC_s) as used in this study. With respect to most of the results from North America and Europe, the upper estimates of the "equivalent MAC" values were typically above 20 $m^2\,g^{-1}$, which was attributed to the artifacts associated with the "filter-based" methods and the enhancement by coating. On the other hand, the "equivalent MAC" values were much lower in India (below 10 $m^2\,g^{-1}$ for two urban sites, Table 1), probably due to the large amounts of brown carbon emitted from biomass burning. This hypothesis was strongly supported by results from North America and Europe such that the reported MAC values were much lower during the periods impacted by biomass burning.

The absorption spectra of WSOC in Beijing was characteristic of the brown carbon spectra with a sharply increasing absorption when wavelength decreases ($\sigma_{abs} \sim \lambda^{-7}$). The σ_{abs} of WSOC (measured at 365 nm) was 1.83 and 0.70 $m^2\,g^{-1}$ during winter and summer respectively. Our previous study demonstrated that WSOC in Beijing was strongly linked to SOA and the SOA to OA ratio was comparable during winter and summer (40% and 50% respectively, Cheng et al., 2011). Moreover, the emission of biogenic volatile organic compounds (BVOCs) in Beijing was approximately 1000 times lower during winter compared with summer, indicating that anthropogenic volatile

ACPD
11, 6221–6258, 2011

organic compounds (AVOCs) should be more important as the precursors of SOA in winter. As a result, the observed seasonal pattern of the σ_{abs} of WSOC was attributed to the difference in the precursors of SOA. The σ_{abs} of WSOC in Beijing was found to be much higher than results from the southeastern United States which were obtained using the same method as used in this study, perhaps due to the influence of biomass burning.

Acknowledgements. This work was supported by the National Natural Science Foundation of China (20625722), the National 973 Program of China (2010CB951803), and the Foundation for the Author of National Excellent Doctoral Dissertation of PR China (2007B57). The authors would like to acknowledge visiting scholar Charles N. Freed for revising the paper, and would also like to acknowledge Chen Lai-guo, Marcus Trail, and Colin Boswell for their help in the analysis.

References

Alexander, D. T. L., Crozier, P. A., and Anderson, J. R.: Brown carbon spheres in East Asian outflow and their optical properties, Science, 321, 833–836, 2008.

Allen, G. A., Lawrence, J., and Koutrakis, P.: Field validation of a semi-continuous method for aerosol black carbon (Aethalometer) and temporal patterns of summertime hourly black carbon measurements in southwestern PA, Atmos. Environ., 33, 817–823, 1999.

Andreae, M. O. and Crutzen, P. J.: Atmospheric aerosols: Biogeochemical sources and role in atmospheric chemistry, Science, 276, 1052–1058, 1997.

Andreae, M. O. and Gelencsér, A.: Black carbon or brown carbon? The nature of light-absorbing carbonaceous aerosols, Atmos. Chem. Phys., 6, 3131–3148, doi:10.5194/acp-6-3131-2006, 2006.

Arnott, W. P., Moosmüller, H., Sheridan, P. J., Ogren, J. A., Raspet, R., Slaton, W. V., Hand, J. L., Kreidenweis, S. M., and Collett, J. L.: Photoacoustic and filter-based ambient aerosol light absorption measurements: instrument comparisons and the role of relative humidity, J. Geophys. Res., 108(D1), 4034, doi:10.1029/2002JD002165, 2003.

Babich, P., Davey, M., Allen, G., and Koutrakis, P.: Method comparisons for particulate nitrate,

ACPD

11, 6221–6258, 2011

elemental carbon, and $PM_{2.5}$ mass in seven US cities, J. Air Waste Manage., 50, 1095–1105, 2000.
Bergstrom, R. W., Ackerman, T. P., and Richards, L. W.: Optical Properties of particulate elemental carbon, in: Particulate carbon: atmospheric life cycle, edited by: Wolff, G. T. and Klimisch, R. L., Plenum Press, New York, 1982.
Bergstrom, R. W., Pilewskie, P., Russell, P. B., Redemann, J., Bond, T. C., Quinn, P. K., and Sierau, B.: Spectral absorption properties of atmospheric aerosols, Atmos. Chem. Phys., 7, 5937–5943, doi:10.5194/acp-7-5937-2007, 2007.
Birch, M. E. and Cary, R. A.: Elemental carbon-based method for monitoring occupational exposures to particulate diesel exhaust, Aerosol Sci. Technol., 25, 221–241, 1996.
Bond, T. C.: Spectral dependence of visible light absorption by carbonaceous particles emitted from coal combustion, Geophys. Res. Lett., 28, 4075–4078, doi:10.1029/2001GL013652, 2001.
Bond, T. C. and Bergstrom, R. W.: Light absorption by carbonaceous particles: an investigative review, Aerosol Sci. Technol., 40, 27–67, 2006.
Bond, T. C., Habib, G., and Bergstrom, R. W.: Limitations in the enhancement of visible light absorption due to mixing state, J. Geophys. Res., 111, D20211, doi:10.1029/2006JD007315, 2006.
Bond, T. C., Streets, D. G., Yarber, K. F., Nelson, S. M., Woo, J. H., and Klimont, Z.: A technology-based global inventory of black and organic carbon emissions from combustion, J. Geophys. Res., D14, D14203, doi:10.1029/2003JD003697, 2004.
Cao, G. L., Zhang, X. Y., and Zheng, F. C.: Inventory of black carbon and organic carbon emissions from China, Atmos. Environ., 40, 6516–6527, 2006.
Chakrabarty, R. K., Moosmüller, H., Garro, M. A., Arnott, W. P., Walker, J., Susott, R. A., Babbitt, R. E., Wold, C. E., Lincoln, E. N., and Hao, W. M.: Emissions from the laboratory combustion of wildland fuels: particle morphology and size, J. Geophys. Res., 111, D07204, doi:10.1029/2005JD006659, 2006.
Chakrabarty, R. K., Moosmüller, H., Chen, L.-W. A., Lewis, K., Arnott, W. P., Mazzoleni, C., Dubey, M. K., Wold, C. E., Hao, W. M., and Kreidenweis, S. M.: Brown carbon in tar balls from smoldering biomass combustion, Atmos. Chem. Phys., 10, 6363–6370, doi:10.5194/acp-10-6363-2010, 2010.
Chen, Y. and Bond, T. C.: Light absorption by organic carbon from wood combustion, Atmos. Chem. Phys., 10, 1773–1787, doi:10.5194/acp-10-1773-2010, 2010.

ACPD
11, 6221–6258, 2011

Cheng, Y., He, K. B., Duan, F. K., Zheng, M., Ma, Y. L., and Tan, J. H.: Positive sampling artifact of carbonaceous aerosols and its influence on the thermal-optical split of OC/EC, Atmos. Chem. Phys., 9, 7243–7256, doi:10.5194/acp-9-7243-2009, 2009.
Cheng, Y., He, K. B., Duan, F. K., Zheng, M., Ma, Y. L., Tan, J. H., and Du, Z. Y.: Improved measurement of carbonaceous aerosol: evaluation of the sampling artifacts and intercomparison of the thermal-optical analysis methods, Atmos. Chem. Phys., 10, 8533–8548, doi:10.5194/acp-10-8533-2010, 2010.
Cheng, Y., He, K. B., Duan, F. K., Zheng, M., Du, Z. Y., Ma, Y. L., and Tan, J. H.: Ambient organic carbon to elemental carbon ratios: influences of the measurement methods and implications, Atmos. Environ., doi:10.1016/j.atmosenv.2011.01.064, 2011.
Chow, J. C., Watson, J. G., Chen, L. A., Arnott, W. P., and Moosmüller, H.: Equivalence of elemental carbon by thermal/optical reflectance and transmittance with different temperature protocols, Environ. Sci. Technol., 38, 4414–4422, 2004.
Chow, J. C., Watson, J. G., Pritchett, L. C., Pierson, W. R., Frazier, C. A., and Purcell, R. G.: The DRI Thermal/Optical Reflectance carbon analysis system: description, evaluation and applications in US air quality studies, Atmos. Environ., 27A, 1185–1201, 1993.
Clarke, A., McNaughton, C., Kapustin, V., Shinozuka, Y., Howell, S., Dibb, J., Zhou, J., Anderson, B., Brekhovskikh, V., Turner, H., and Pinkerton, M.: Biomass burning and pollution aerosol over North America: organic components and their influence on spectral optical properties and humidification response, J. Geophys. Res., 112, D12S18, doi:10.1029/2006JD007777, 2007.
Duan, F. K., Liu, X. D., Yu, T., and Cachier, H.: Identification and estimate of biomass burning contribution to the urban aerosol organic carbon concentrations in Beijing, Atmos. Environ., 38, 1275–1282, 2004.
Gelencsér, A., Hoffer, A., Kiss, G., Tombácz, E., Kurdi, R., and Bencze, L.: In-situ formation of light-absorbing organic matter in cloud water, J. Atmos. Chem., 45, 25–33, 2003.
Gustafsson, O., Kruså, M., Zencak, Z., Sheesley, R. J., Granat, L., Engström, E., Praveen, P. S., Rao, P. S. P., Leck, C., and Rodhe, H.: Brown clouds over south Asia: biomass or fossil fuel combustion?, Science, 323, 495–498, 2009.
Hand, J. L., Malm, W. C., Laskin, A., Day, D., Lee, T., Wang, C., Carrico, C., Carrillo, J., Cowin, J. P., Collett, J., and Iedema, M. J.: Optical, physical, and chemical properties of tar balls observed during the Yosemite Aerosol Characterization Study, J. Geophys. Res., 110, D21210, doi:10.1029/2004JD005728, 2005.

ACPD
11, 6221–6258, 2011

Hansen, A. D. A. and Novakov, T.: Real-time measurement of aerosol black carbon during the carbonaceous species methods comparison study, Aerosol Sci. Technol., 12, 194–199, 1990.
He, L. Y., Hu, M., Huang, X. F., Zhang, Y. H., and Tang, X. Y.: Seasonal pollution characteristics of organic compounds in atmospheric fine particles in Beijing, Sci. Total. Environ., 359, 167–176, 2006.
Hecobian, A., Zhang, X., Zheng, M., Frank, N., Edgerton, E. S., and Weber, R. J.: Water-Soluble Organic Aerosol material and the light-absorption characteristics of aqueous extracts measured over the Southeastern United States, Atmos. Chem. Phys., 10, 5965–5977, doi:10.5194/acp-10-5965-2010, 2010.
Hoffer, A., Gelencsr, A., Guyon, P., Kiss, G., Schmid, O., Frank, G. P., Artaxo, P., and Andreae, M. O.: Optical properties of humic-like substances (HULIS) in biomass-burning aerosols, Atmos. Chem. Phys., 6, 3563–3570, doi:10.5194/acp-6-3563-2006, 2006.
Husain, L., Dutkiewicz, V. A., Khan, A., and Ghauri, B. M.: Characterization of carbonaceous aerosols in urban air, Atmos. Environ., 41, 6872–6883, 2007.
Jacobson, M. Z.: Isolating nitrated and aromatic aerosols and nitrated aromatic gases as sources of ultraviolet light absorption, J. Geophys. Res., 104, 3527–3542, doi:10.1029/1998JD100054, 1999.
Jacobson, M. Z.: Strong radiative heating due to the mixing state of black carbon in atmospheric aerosols, Nature, 409, 695–697, 2001.
Jeong, C. H., Hopke, P. K., Kim, E., and Lee, D. W.: The comparison between thermal-optical transmittance elemental carbon and Aethalometer black carbon measured at multiple monitoring sites, Atmos. Environ., 38, 5193–5204, 2004.
Kirchstetter, T. W., Novakov, T., and Hobbs, P. V.: Evidence that the spectral dependence of light absorption by aerosols is affected by organic carbon, J. Geophys. Res., 109, D21208, doi:10.1029/2004JD004999, 2004.
Knox, A., Evans, G. J., Brook, J. R., Yao, X., Jeong, C. H., Godri, K. J., Sabaliauskas, K., and Slowik, J. G.: Mass absorption cross-section of ambient black carbon aerosol in relation to chemical age, Aerosol Sci. Technol., 43, 522–532, 2009.
Krecl, P., Strom, J., and Johansson, C.: Carbon content of atmospheric aerosols in a residential area during the wood combustion season in Sweden, Atmos. Environ., 41, 6974–6985, 2007.
Li, W. J., Shao, L. Y., and Buseck, P. R.: Haze types in Beijing and the influence of agricul-

ACPD
11, 6221–6258, 2011

tural biomass burning, Atmos. Chem. Phys., 10, 8119–8130, doi:10.5194/acp-10-8119-2010, 2010.
Lim, H. J., Turpin, B. J., Edgerton, E., Hering, S. V., Allen, G., Maring, H., and Solomon, P.: Semicontinuous aerosol carbon measurements: comparison of Atlanta Supersite measurements, J. Geophys. Res., 108(D7), 8419, doi:10.1029/2001JD001214, 2003.
Liousse, C., Cachier, H., and Jennings, S. G.: Optical and thermal measurements of black carbon aerosol content in different environments: variation of the specific attenuation cross-section, sigma (σ), Atmos. Environ., 27A, 1203–1211, 1993.
Lukács, H., Gelencsér, A., Hammer, S., Puxbaum, H., Pio, C., Legrand, M., Kasper-Giebl, A., Handler, M., Limbeck, A., Simpson, D., and Preunkert, S.: Seasonal trends and possible sources of brown carbon based on 2-year aerosol measurements at six sites in Europe, J. Geophys. Res., 112, D23S18, doi:10.1029/2006JD008151, 2007.
Menon, S., Hansen, J., Nazarenko, L., and Luo, Y. F.: Climate effects of black carbon aerosols in China and India, Science, 297, 2250–2253, 2002.
Petzold, A., Schloesser, H., Sheridan, P. J., Arnott, W. P., Ogren, J. A., and Virkkula, A.: Evaluation of multiangle absorption photometry for measuring aerosol light absorption, Aerosol Sci. Technol., 39, 40–51, 2005.
Pöschl, U.: Atmospheric aerosols: composition, transformation, climate and health effects, Angew. Chem. Int. Ed., 44, 7520–7540, 2005.
Pósfai, M., Gelencsér, A., Simonics, R., Arató, K., Li, J., Hobbs, P. V., and Buseck, P. R.: Atmospheric tar balls: particles from biomass and biofuel burning, J. Geophys. Res., 109, D06213, doi:10.1029/2003JD004169, 2004.
Quincey, P., Butterfield, D., Green, D., Coyle, M., and Cape, C. N.: An evaluation of measurement methods for organic, elemental and black carbon in ambient air monitoring sites, Atmos. Environ., 43, 5085–5091, 2009.
Ram, K. and Sarin, M. M.: Absorption coefficient and site-specific mass absorption efficiency of elemental carbon in aerosols over urban, rural, and high-altitude sites in India, Environ. Sci. Technol., 43, 8233–8239, 2009.
Ramanathan, V. and Carmichael, G.: Global and regional climate changes due to black carbon, Nat. Geosci., 1, 221-227, 2008.
Ramanathan, V., Crutzen, P. J., Kiehl, J. T., and Rosenfeld, D.: Aerosols, climate, and the hydrological cycle, Science, 294, 2119–2124, 2001.
Rattigan, O. V., Dirk Felton, H., Bae, M. S., Schwab, J. J., and Demerjian, K. L.: Multi-year

ACPD
11, 6221–6258, 2011

hourly $PM_{2.5}$ carbon measurements in New York: diurnal, day of week and seasonal patterns, Atmos. Environ., 44, 2043–2053, 2010.
Reisinger, P., Wonaschütz, A., Hitzenberger, R., Petzold, A., Bauer, H., Jankowski, N., Puxbaum, H., Chi, X., and Maenhaut, W.: Intercomparison of measurement techniques for black or elemental carbon under urban background conditions in wintertime: influence of biomass combustion, Environ. Sci. Technol., 42, 884–889, 2008.
Rice, J.: Comparison of integrated filter and automated carbon aerosol measurements at research triangle park, North Carolina, Aerosol Sci. Technol., 38, 23–36, 2004.
Weber, R. J., Sullivan, A. P., Peltier, R. E., Russell, A., Yan, B., Zheng, M., de Gouw, J., Warneke, C., Brock, C., Holloway, J. S., Atlas, E. L., and Edgerton, E.: A study of secondary organic aerosol formation in the anthropogenic-influenced southeastern United States, J. Geophys. Res., 112, D13302, doi:10.1029/2007JD008408, 2007.
Sandradewi, J., Prevot, A. S. H., Weingartner, E., Schmidhauser, R., Gysel, M., and Baltensperger, U.: A study of wood burning and traffic aerosols in an Alpine valley using a multi-wavelength Aethalometer, Atmos. Environ., 42, 101–112, 2008.
Schauer, J. J., Mader, B. T., DeMinter, J. T., Heidemann, G., Bae, M. S., Seinfeld, J. H., Flagan, R, C., Cary, R. A., Smith, D., Huebert, B. J., Bertram, T., Howell, S., Kline, J. T., Quinn, P., Bates, T., Turpin, B., Lim, H. J., Yu, J. Z., Yang, H., and Keywood, M. D.: ACE-Asia intercomparison of a thermal-optical method for the determination of particle-phase organic and elemental carbon, Environ. Sci. Technol., 37, 993–1001, 2003.
Schnaiter, M., Horvath, H., Möhler, O., Naumann, K. H., Saathoff, H., and Schöck, O. W.: UV-VIS-NIR spectral optical properties of soot and soot-containing aerosols, J. Aerosol Sci., 34, 1421–1444, 2003.
Schnaiter, M., Linke, C., Möhler, O., Naumann, K. H., Saathoff, H., Wagner, R., Schurath, U., and Wehner, B.: Absorption amplification of black carbon internally mixed with secondary organic aerosol, J. Geophys. Res., 110, D19204, doi:10.1029/2005JD006046, 2005.
Schnaiter, M., Gimmler, M., Llamas, I., Linke, C., Jäger, C., and Mutschke, H.: Strong spectral dependence of light absorption by organic carbon particles formed by propane combustion, Atmos. Chem. Phys., 6, 2981–2990, doi:10.5194/acp-6-2981-2006, 2006.
Sciare, J., Cachier, H., Oikonomou, K., Ausset, P., Sarda-Estéve, R., and Mihalopoulos, N.: Characterization of carbonaceous aerosols during the MINOS campaign in Crete, July-August 2001: a multi-analytical approach, Atmos. Chem. Phys., 3, 1743–1757, doi:10.5194/acp-3-1743-2003, 2003.

ACPD
11, 6221–6258, 2011

Sharma, S, Brook, J. R., Cachier, H., Chow, J., Gaudenzi, A., and Lu, G.: Light absorption and thermal measurements of black carbon in different regions of Canada, J. Geophys. Res., 107(D24), 4771, doi:10.1029/2002JD002496, 2002.

Snyder, D. C. and Schauer, J. J.: An inter-comparison of two black carbon aerosol instruments and a semi-continuous elemental carbon instrument in the urban environment, Aerosol Sci. Technol., 41, 463–474, 2007.

Snyder, D. C., Rutter, A. P., Collins, R., Worley, C., and Schauer, J. J.: Insights into the origin of water soluble organic carbon in atmospheric fine particulate matter, Aerosol Sci. Technol., 43, 1099–1107, 2009.

Subramanian, R., Khlystov, A. Y., and Robinson, A. L.: Effect of peak inert-mode temperature on elemental carbon measured using thermal-optical analysis, Aerosol Sci. Technol., 40, 763–780, 2006.

Sullivan, A. P., Weber. R. J., Clements, A. L., Turner, J. R., Bae, M. S., and Schauer, J. J.: A method for on-line measurement of water-soluble organic carbon in ambient aerosol particles: results from an urban site, Geophys. Res. Lett., 31, L13105, doi:10.1029/2004GL019681, 2004.

van Poppel, L. H., Friedrich, H., Spinsby, J., Chung, S. H., Seinfeld, J. H., and Buseck, P. R. Electron tomograohy of nanoparticle clusters: implications for atmospheric lifetimes and radiative forcing of soot, Geophys. Res. Lett., 32, L24811, doi:10.1029/2005GL024461, 2005.

Venkatachari, P., Zhou, L. M., Hopke, P. K., Schwab, J. J., Demerjian, K. L., Weimer, S., Hogrefe, O., Felton, D., and Rattigan, O.: An intercomparison of measurement methods for carbonaceous aerosol in the ambient air in New York City, Aerosol Sci. Technol., 40, 788–795, 2006.

Venkataraman, C., Habib, G., Eiguren-Fernandez, A., Miguel, A. H., and Friedlander, S. K.: Residential biofuels in south Asia: carbonaceous aerosol emissions and climate impacts, Science, 307, 1454–1456, 2005.

Wang, Q., Shao, M., Zhang, Y., Wei, Y., Hu, M., and Guo, S.: Source apportionment of fine organic aerosols in Beijing, Atmos. Chem. Phys., 9, 8573–8585, 2009, http://www.atmos-chem-phys.net/9/8573/2009/.

Wang, Z. H., Bai, Y. H., and Zhang S. Y.: A biogenic volatile organic compounds emission inventory for Beijing, Atmos. Environ., 37, 3771–3782, 2003.

Weingartner, E., Saathoff, H., Schnaiter, M., Streit, N., Bitnar, B., and Baltensperger, U.: Absorption of light by soot particles: determination of the absorption coefficient by means of

ACPD
11, 6221–6258, 2011

Aethalometers, J. Aerosol Sci., 34, 1445–1463, 2003.
Zhang, T., Claeys, M., Cachier, H., Dong, S. P., Wang, W., Maenhaut, W., and Liu, X. D.: Identification and estimation of the biomass burning contribution to Beijing aerosol using levoglucosan as a molecular marker, Atmos. Environ., 42, 7013–7021, 2008.
Zhang, X., Hecobian, A., Zheng, M., Frank, N. H., and Weber, R. J.: Biomass burning impact on $PM_{2.5}$ over the southeastern US during 2007: integrating chemically speciated FRM filter measurements, MODIS fire counts and PMF analysis, Atmos. Chem. Phys., 10, 6839–6853, doi:10.5194/acp-10-6839-2010, 2010.

ACPD
11, 6221–6258, 2011

Table 1. Previously published mass absorption cross-section (MAC, in $m^2\,g^{-1}$) of elemental carbon (EC). The lower and upper estimates of the "equivalent MAC", which is the estimated value if using the same measurement methods as used in this study, are also shown.

Sampling site	Sample description	Methods of b_{abs}[a]	Methods of EC	Reported MAC	Equivalent MAC		Reference
					Lower	Upper	
Group 1							
Philadelphia, PA	Severe sulfate haze episodes	Aethalometer (880 nm)	NIOSH (TOT)[b]	59.9	55.6	69.5	Jeong et al. (2004)
Riverside, CA	Urban, summer	Aethalometer (880 nm)	IMPROVE (TOR)[c]	15.8	28.5	39.5	Babich et al. (2000)
New York	Urban, April to September	Aethalometer (880 nm)	NIOSH (TOT)	33.2	30.8	38.5	Rattigan et al. (2010)
Chicago, IL	Urban, autumn	Aethalometer (880 nm)	IMPROVE (TOR)	14.4	26.1	36.2	Babich et al. (2000)
Phoenix, AZ	Urban, winter	Aethalometer (880 nm)	IMPROVE (TOR)	13.5	24.4	33.8	Babich et al. (2000)
Beijing, China	Urban, summer	DRI analyzer (632 nm)	IMPROVE-A (TOT)[d]	32.0			This study
Bakersfield, CA	Urban, winter	Aethalometer (880 nm)	IMPROVE (TOR)	12.0	21.7	30.0	Babich et al. (2000)
Dallas, TX	Urban, winter	Aethalometer (880 nm)	IMPROVE (TOR)	11.8	21.3	29.5	Babich et al. (2000)
Philadelphia, PA	Urban, summer	Aethalometer (880 nm)	IMPROVE (TOR)	11.8	21.3	29.5	Babich et al. (2000)
Beijing, China	Urban, winter	DRI analyzer (632 nm)	IMPROVE-A (TOT)	29.0			This study
New York	Urban, October to March	Aethalometer (880 nm)	NIOSH (TOT)	23.2	21.6	27.0	Rattigan et al. (2010)
Group 2							
Scotland, UK	Rural, June to December	Aethalometer (880 nm)	NIOSH (TOT)	22.1	20.5	25.6	Quincey et al. (2009)
Atlanta, GA	Urban, summer	Aethalometer (880 nm)	NIOSH (TOT)	20.4	19.0	23.7	Lim et al. (2003)
Evans, Canada	Urban, winter	Aethalometer (880 nm)	MSC (TOT)[e]	9.5	18.7[f]	26.0[f]	Sharma et al. (2002)
Toronto, Canada	Urban, annual	Aethalometer (880 nm)	NIOSH (TOT)	19.7	18.3	22.9	Knox et al. (2009)
Durham, NC	Urban, summer	Aethalometer (880 nm)	NIOSH (TOT)	19.4	18.0	22.5	Rice (2004)
Riverside, CA	Urban, summer	Aethalometer (880 nm)	NIOSH (TOT)	18.5	17.2	21.5	Snyder and Schauer (2007)
Egbert, Canada	Rural, summer	Aethalometer (880 nm)	IMPROVE (TOR)	8.7	15.7	21.8	Sharma et al. (2002)
Palmerston, Canada	Urban, summer	Aethalometer (880 nm)	MSC (TOT)	7.5	14.8[f]	20.5[f]	Sharma et al. (2002)

ACPD
11, 6221–6258, 2011

Table 1. Continued.

Sampling site	Sample description	Methods of b_{abs}^{a}	Methods of EC	Reported MAC	Equivalent MAC		Reference
					Lower	Upper	
Group 3							
Lahore, Pakistan	Urban, winter	Aethalometer (880 nm)	NIOSH (TOT)	20.8		19.3[g]	Husain et al. (2007)
Manora Peak, India	High altitude, winter	Sunset analyzer (678 nm)	NIOSH (TOT)	24.7		17.7[g]	Ram and Sarin (2009)
Lycksele, Sweden	Urban, wood burning season	Aethalometer (880 nm)	NIOSH (TOT)	13.4	12.5	15.6	Krecl et al. (2007)
Mt. Abu, India	High altitude, winter	Sunset analyzer (678 nm)	NIOSH (TOT)	16.4		11.7[g]	Ram and Sarin, 2009
Uniontown, PA	Sub-urban, summer influenced by open burning	Aethalometer (530 nm)	IMPROVE (TOR)	7.5	8.2	11.3	Allen et al. (1999)
Hisar, India	Urban, winter	Sunset analyzer (678 nm)	NIOSH (TOT)	12.8		9.2[g]	Ram and Sarin (2009)
Allahabad, India	Urban, winter	Sunset analyzer (678 nm)	NIOSH (TOT)	11.1		7.9[g]	Ram and Sarin (2009)
Philadelphia, PA	Canadian forest fire event	Aethalometer (880 nm)	NIOSH (TOT)	5.8	5.4	6.7	Jeong et al. (2004)

[a] The operating-wavelength shown in parentheses.
[b] NIOSH temperature protocol with transmittance correction.
[c] IMPROVE temperature protocol with reflectance correction.
[d] IMPROVE-A temperature protocol with transmittance correction.
[e] MSC (Meteorological Service of Canada) temperature protocol with transmittance correction.
[f] EC determined by the MSC method was 1.09 times the value of that determined by the IMPROVE temperature protocol with reflectance correction (Sharma et al., 2002). In Eq. (10), $f_{charring} = (1.3 \sim 1.8) \times 1.09$, $f_{protocol} = 1$.
[g] The upper estimate of "equivalent MAC" calculated by a $f_{protocol}$ value of 1.5.

ACPD
11, 6221–6258, 2011

Table 2. Ratios of reflectance-defined EC (EC_R) to transmittance-defined EC (EC_T).

Protocol	Sampling site	Sample description	Ratio	Reference
IMPROVE	Multiple, US	Urban, sub-urban, and rural	1.78	Chow et al. (2001)
IMPROVE	Multiple, Mexico	Urban	1.47	Chow et al. (2001)
IMPROVE	Fresno, CA	Aug 2002–Apr 2003; urban	1.49	Chow et al. (2004)
IMPROVE	Fresno, CA	Aug–Sep 2005; urban	1.33	Chow et al. (2009)
IMPROVE-A	Beijing, China	Winter and summer, 2009; urban	1.78	Cheng et al. (2010)
IMPROVE	–	Motor vehicle exhaust; source	1.21	Chow et al. (2001)
NIOSH	Multiple, Mexico	Urban	1.00	Chow et al. (2001)
STN	Fresno, CA	Aug 2002–Apr 2003; urban	3.45	Chow et al. (2004)
STN	Hong Kong, China	Nov 2000–Oct 2001; urban	1.16	Chow et al. (2005)

ACPD
11, 6221–6258, 2011

Table 3. Lower and upper estimates of the "equivalent MAC" values before and after correction for the artifacts associated with the "filter-based" method (an enhancement factor of 1.87 was used).

	Equivalent MAC uncorrected		Equivalent MAC corrected		Note
	Lower	Upper	Lower	Upper	
Group 1	21 ~ 31	27 ~ 40	11 ~ 17	14 ~ 21	Significantly enhanced by coating
Group 2	15 ~ 21	21 ~ 26	8 ~ 11	11 ~ 14	Moderately enhanced by coating
Group 3		<20		<11	Impacted by biomass burning

ACPD
11, 6221–6258, 2011

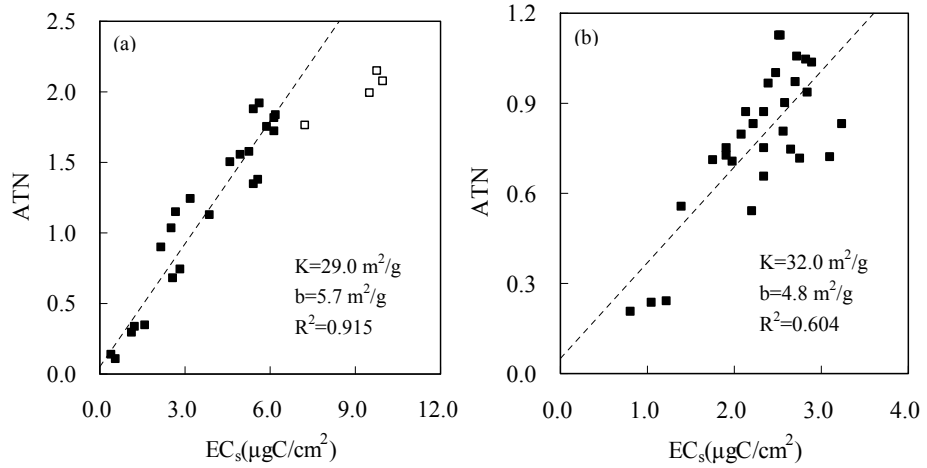

Fig. 1. Comparison of light attenuation measured at 632 nm (ATN) and EC loading (EC_s) during winter **(a)** and summer **(b)** respectively. Linear regression results are shown with K as the slope and b as the intercept. Data points with ECs exceeding 7 μgC cm^{-2}, as shown by the open squares, were not included in the regression to avoid the shadowing effect.

ACPD
11, 6221–6258, 2011

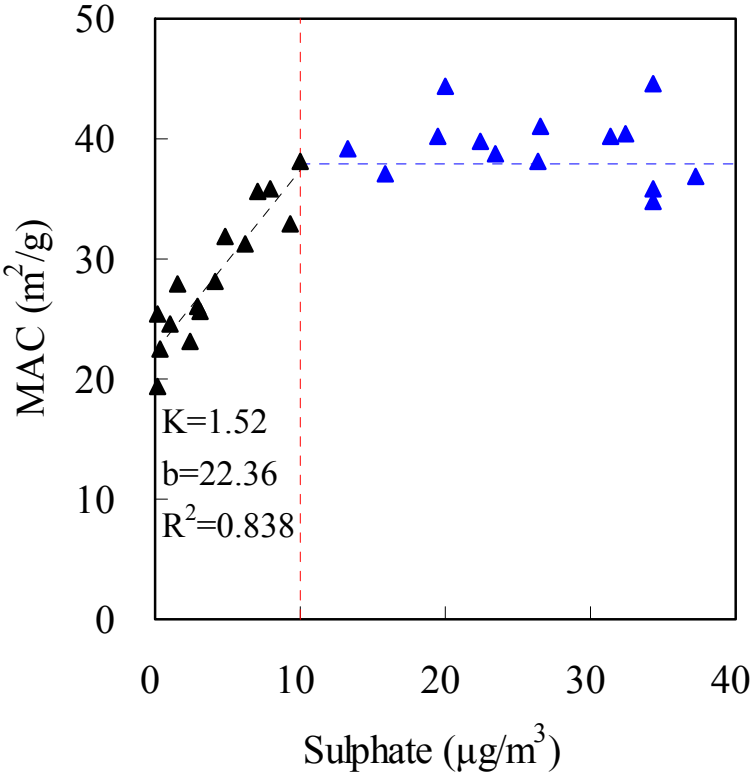

Fig. 2. Relationship between the MAC of EC and the sulphate concentration during summer. Linear regression results are shown with K as the slope and b as the intercept. The linearity did not extend for sulphate exceeding 10 μg m^{-3}, as indicated by the red dash line. The trend was similar during winter.

ACPD
11, 6221–6258, 2011

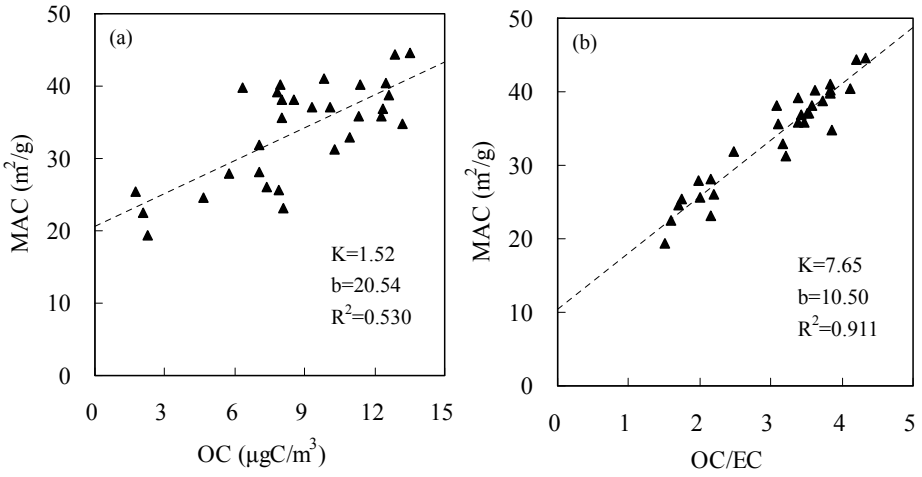

Fig. 3. Relationship between the MAC of EC and **(a)** the OC concentration, **(b)** the OC to EC ratio (OC/EC) during summer. Linear regression results are shown with *K* as the slope and *b* as the intercept. The trend was similar during winter.

ACPD
11, 6221–6258, 2011

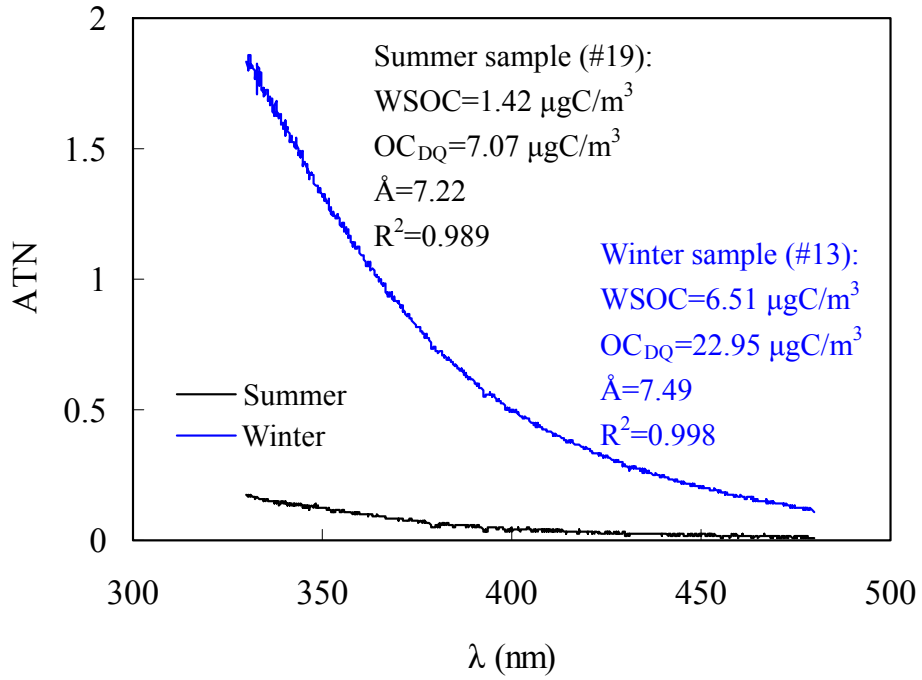

Fig. 4. Representative adsorption spectra of WSOC during winter and summer respectively.

ACPD
11, 6221–6258, 2011

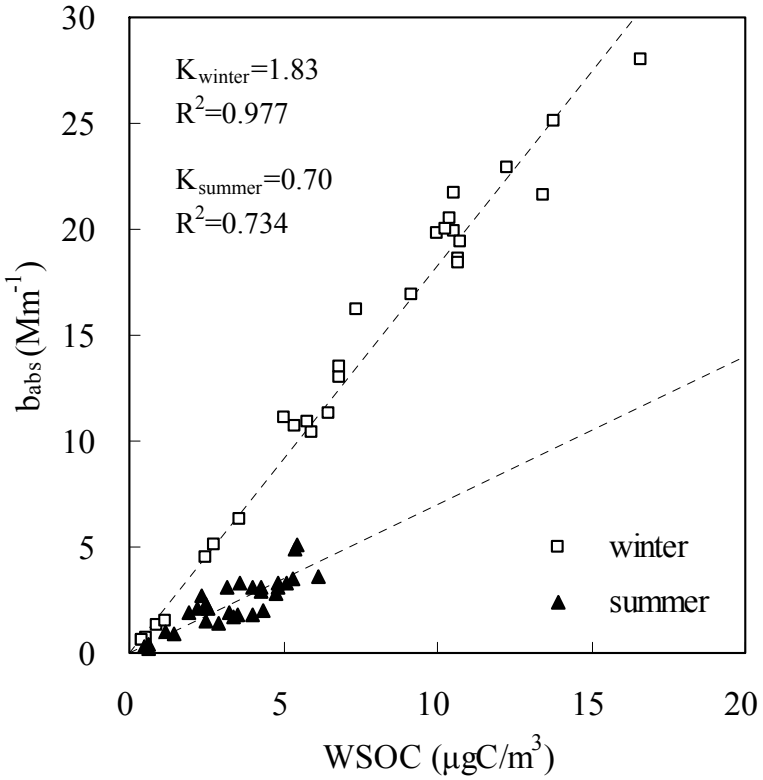

Fig. 5. Comparison of b_{abs} measured at 365 nm and the WSOC concentration during winter and summer. Linear regression results are shown with K as the slope (intercept is set as zero).

ACPD
11, 6221–6258, 2011